SSCL-540
RU 91/15/B
Fermilab-Pub-91/261

SSCL-540
RU 91/15/B
Fermilab-Pub-91/261

Superconducting Super Collider Laboratory

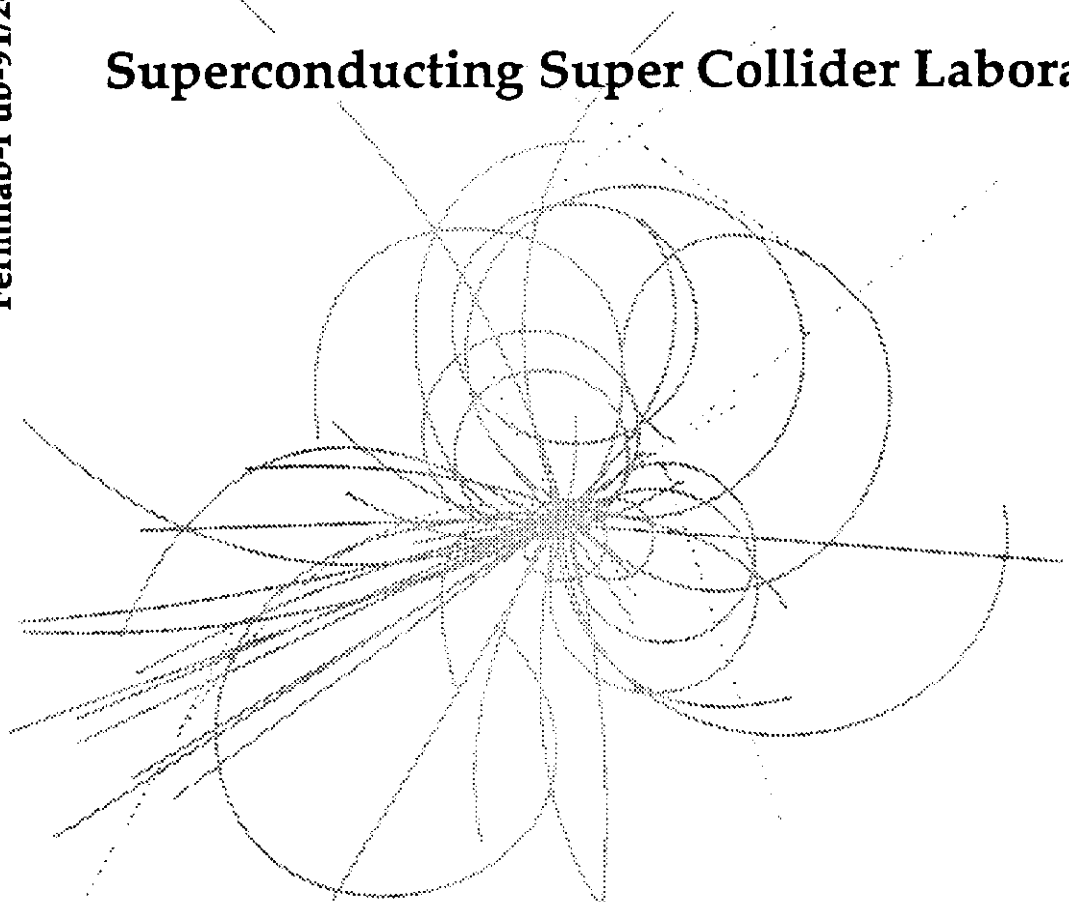

Is There a P-Wave Bound State of W_LW_L?

Atkinson et al.

October 1991

SSCL-540
RU 91/15/B
Fermilab-Pub-91/261

Is There a P-Wave Bound State of $W_L W_L$?
On the Dynamical Generation of a ρ Meson in the σ Model

D. Atkinson

Fermi National Laboratory
P.O. Box 500
Batavia, IL 60510
U.S.A.

and

Institute for Theoretical Physics
P.O.Box 800
9700 AV Groningen
The Netherlands

M. Harada

Department of Physics
Nagoya University
Nagoya 464-01
Japan

A. I. Sanda

Superconducting Super Collider Laboratory*
2550 Beckleymeade Avenue
Dallas, TX 75237

and

Department of Physics
Rockefeller University
New York, N. Y. 10021

October 1991

* This work was supported by the Universities Research Association, Inc., for the U.S. Department of Energy under Contract No. DE-AC35-89ER40486.

SSCL-540
RU 91/15/B
Fermilab-Pub-91/261

Is There a P-Wave Bound State of $W_L W_L$?
On the Dynamical Generation of a ρ Meson in the σ Model

D. Atkinson, M. Harada, and A. I. Sanda

Abstract

We investigate the possibility that the Higgs lagrangian predicts the existence of a P-wave $W_L W_L$ resonance. This problem is equivalent to studying the formation of the ρ meson by the dynamics contained in the σ model. Using the Padé approximation, Basdevant and Lee had claimed that ρ is generated dynamically. We show that their result, while computationally correct, is not significant, because of the position of the Landau ghost. For the same reason, a $W_L W_L$ P-wave resonance below 2 TeV is not expected, **unless the standard model is violated.**

1.0 INTRODUCTION

It is by now generally accepted that the gauge sector of the standard model, based on the $SU(2) \otimes U(1)$ gauge group, agrees extremely well with experiment. What is not tested at all, in this very successful electroweak theory, is the mechanism for breaking the symmetry spontaneously. It is likely that the next major advance in high energy physics will come from discovering which mechanism nature has chosen.

The Superconducting Super Collider (SSC) is being built to study this symmetry breaking. The first item on the agenda is the Higgs boson search. The electroweak theory, however, does not constrain the mass of the Higgs. If this mass is below 800 GeV, SSC should be able to see the Higgs, but if the mass is larger, direct detection will be impossible.

We ask what is the best strategy for SSC to study the symmetry breaking, should the Higgs boson be too heavy for straightforward detection as an S-wave resonance. For definiteness, we limit ourselves to the minimal standard model Higgs lagrangian. We then look for the predictions that can be experimentally checked.

Our starting point is the well known isomorphism between the Higgs lagrangian and the σ model. The longitudinal components of W bosons correspond, in this isomorphism, to π mesons. The Higgs boson corresponds to the σ. If the coupling of L_H is as strong as that of L_σ, the Higgs will not be seen at all! After all, since σ is so broad, there are serious doubts as to its existence as a second-sheet pole of the $\pi\pi$ scattering amplitude. On the other hand, nobody doubts the existence of the ρ. Could it be that a P-wave resonance of the longitudinal W's will be found instead of the Higgs itself? We can try to answer this question by looking at the $\pi\pi$ case and investigating the nature of the ρ meson.

At this point, the reader may wonder if all this is necessary. The lattice analysis gives the following bounds:[1]

$$m_{\text{Higgs}}(F_4 < 0.3\%) < 530 \pm 60\,\text{GeV}$$
$$m_{\text{Higgs}}(F_4 < 3.0\%) < 590 \pm 60\,\text{GeV}\ ,$$

where the first bound applies if one requires that the F_4 lattice cutoff effect is no larger than 0.3%, whereas the second bound is applicable if one tolerates a 3.0% cutoff effect. These bounds imply that if the Higgs boson does not satisfy them, then new physics (beyond the standard model) is guaranteed at about this energy.[2] We note that these bounds are too stringent: they correspond to $m_\sigma < 204\ (227)\,\text{MeV}$. Experimentally, m_σ does NOT satisfy them. Thus we conclude that L_σ is not the fundamental theory which governs pion dynamics. Nevertheless, L_σ describes the pion physics below 300 MeV so well that we don't

learn anything about the *new physics*, namely QCD, from the low energy experiments. In the Higgs sector, we may be in the same situation. The Higgs' mass could violate the bound. Yet, no new physics effect may show up in the energy region given by the triviality bound—the relevance of the lattice pronunciamento must be called into doubt on purely experimental grounds.

We expect that L_σ is a low energy effective theory of QCD. But the region of its validity may be confined to a very low energy region. *Perturbatively,* it cannot explain $\pi\pi$ dynamics in the energy region below 1 GeV. There is namely a P-wave resonance, the ρ particle, which is not contained in the perturbative spectrum of the σ model. There are two possibilities:

1. Some nonperturbative dynamics contained in L_σ generates the ρ. One might guess, in this case, that L_σ can generate all observed phenomena in $\pi\pi$ scattering, at least until $K\overline{K}$ effects become significant.

2. The existence of ρ in $\pi\pi$ scattering is due to a remnant of the underlying QCD dynamics, i.e. ρ is predominantly a bound state of $q\bar{q}$, and an effective lagrangian governing the dynamics of ρ has to be added separately.[3]

That is to say, if the dynamics required to bind the ρ meson is already present in L_σ (a low energy effective theory of QCD), then L_H too should generate a P-wave WW resonance, while the origin of L_H does not need to be specified. On the contrary, if ρ is mainly a $q\bar{q}$ bound state not implicitly contained in L_σ, QCD is required to account for the properties of ρ. In this case, if it turns out experimentally that there is a P-Wave WW bound-state, we would have to conclude that physics beyond the standard model is playing an essential role.[4]

In this paper, we shall investigate the possible existence of resonances in the Higgs sector of the standard model. The pion dynamics observed in nature, as well as past theoretical studies of L_σ, can be used to analyze the Higgs and W interactions when the coupling is large—i.e. when the Higgs is heavy.

Twenty years ago, Basdevant and Lee[5] (BL) claimed that the dynamics implied by L_σ generates a resonance in the P-wave amplitude. Using a Padé approximant, they obtained

$$\begin{aligned} m_\rho &= 760 \text{ MeV} \\ \Gamma_\rho &= 35 \text{ MeV}. \end{aligned} \tag{1}$$

This result, if true, would imply that L_H, when the Higgs is heavy, generates a resonance in WW scattering. Furthermore, it is likely to be narrow, and therefore it would be easier to

find than the Higgs boson itself. Its existence would have a profound consequence for SSC experiments. However, we shall show below that, while this BL result can be reproduced numerically, it is an artifact of the Padé approximant.

Two years ago, Dawson and Willenbrock[6] (DW) studied L_H to one loop level. The renormalization prescriptions of BL and DW are quite different. For example, BL define λ at m_π while DW define m_H on its mass shell. As a check on our results, each computation will be done independently in these two renormalization schemes.

2.0 PRELIMINARIES

2.1 Higgs Lagrangian

It has been widely recognized that the Higgs Lagrangian is isomorphic to the $O(4)$ σ model lagrangian. For completeness, we describe the isomorphism here.

The Higgs lagrangian is written in terms of the $SU(2)_L$ doublet

$$\phi = \begin{pmatrix} \phi^+ \\ \phi^0 \end{pmatrix} = \frac{1}{\sqrt{2}} \begin{pmatrix} \phi_1^+ + i\phi_2^+ \\ \phi_1^0 + i\phi_2^0 \end{pmatrix}. \tag{2}$$

The $SU(2) \otimes U(1)$ symmetry breaking is caused by the Lagrangian

$$L_H = \partial_\mu \phi^\dagger \partial^\mu \phi + \tfrac{1}{2}\mu^2 \phi^\dagger \phi \; - \; \lambda(\phi^\dagger \phi)^2. \tag{3}$$

This lagrangian has an $O(4)$ symmetry, as it is invariant under a rotation among $(\phi_1^+, \phi_2^+, \phi_1^0, \phi_2^0)$. In terms of the vacuum expectation value v,

$$L_H = \; \tfrac{1}{2}\partial_\mu \vec{\omega} \cdot \partial^\mu \vec{\omega} \; + \; \tfrac{1}{2}\partial_\mu H \partial^\mu H \; - \; \lambda v^2 H^2 - \lambda v H[\vec{\omega} \cdot \vec{\omega} + H] \; - \; \tfrac{1}{4}\lambda[\vec{\omega} \cdot \vec{\omega} + H]^2 \tag{4}$$

where we identified

$$\phi_1^+ = \omega_1, \;\; \phi_2^+ = \omega_2, \;\; \phi_2^0 = \omega_3, \;\; \phi_1^0 = v + H.$$

The Higgs mass is $m_H^2 = 2\lambda v^2$. Now note that if we make the identification

$$\vec{\omega} \leftrightarrow \vec{\pi}, \;\; H \leftrightarrow \sigma,$$

L_H becomes the linear σ model lagrangian. In the σ model, the $\vec{\pi}$'s are the pseudoscalar Nambu-Goldstone bosons associated with chiral symmetry breaking. When ϕ_1^0 acquires a

vacuum expectation value, the gauge bosons become massive and $\vec{\omega}$ turns into the longitudinal components of the gauge boson. In L_σ and L_H, the energy scale is set by v. For L_σ, $v = f_\pi = 93\,\mathrm{MeV}$, the pion decay constant. For L_H, $v = 2^{-\frac{1}{4}} G_F^{-\frac{1}{2}} = 246\,\mathrm{GeV}$, where G_F is the Fermi coupling constant. Since v is the only energy scale appearing in the theory, the Higgs mass bound given in the introduction can be translated into the σ mass bound by means of a scaling factor $f_\pi(\sqrt{2}G_F)^{\frac{1}{2}}$. Because of this isomorphism, it is clear that both BL and DW actually computed one-loop corrections to the same processes.

2.2 How good is the σ model below 1 GeV?

The σ model was introduced to study the consequences of chiral symmetry, and to translate the results of current algebra into a field theory language. While it should describe the physics of the $\pi\pi$ interaction at low energy, its validity at high energy is not guaranteed. This is particularly true if the coupling λ is large, so that the usefulness of the perturbative expansion is in question. BL have introduced the Padé approximation of the partial-wave amplitudes to remedy the lack of convergence of the perturbation series. They point out that the unitarity constraint is preserved in this approximation.

Before we go into the details of our computation, we wish to show that the σ model, together with the Padé approximation, gives a reasonably satisfactory description of the S-wave $I = 0$ and 2 $\pi\pi$ phase-shifts below 1 GeV. Although the σ is no longer classified as a resonance, the $I = 0$ S-wave phase-shift passes through $\frac{\pi}{2}$ at 858 MeV. By choosing $\frac{m_H}{v} = \frac{858}{93} = 9.23$, we can ensure that the σ model result has an S-wave resonance at this point. In Figure 1 we show the experimental $I = 0$ and $I = 2$ S-wave phase-shifts, up to 1 GeV[10] (dotted lines). The corresponding output of the [1,1] Padé calculation is also shown (solid lines). For comparison purposes, we chose the parameters $f_\pi = 125\,\mathrm{MeV}$, and $\lambda = 5.63$, the values used by Basdevant and Lee,[5] but very similar results can be obtained by setting $f_\pi = 93\,\mathrm{MeV}$. The agreement of these phase-shifts may be said to be reasonable up to 900 MeV, although our threshold behavior seems to be different from that of the interpolation by Roy's equation. Above 0.9 GeV, the $K\overline{K}$ threshold opens up, and the experimental phase-shift shoots up through and beyond $\frac{3\pi}{2}$ [the $f_0(1400)$ resonance]. This is not accounted for in the σ model. With this discussion, we conclude that the [1,1] Padé approximation to σ model predictions at the one loop level is reasonably trustworthy in the energy region below about 1 GeV.

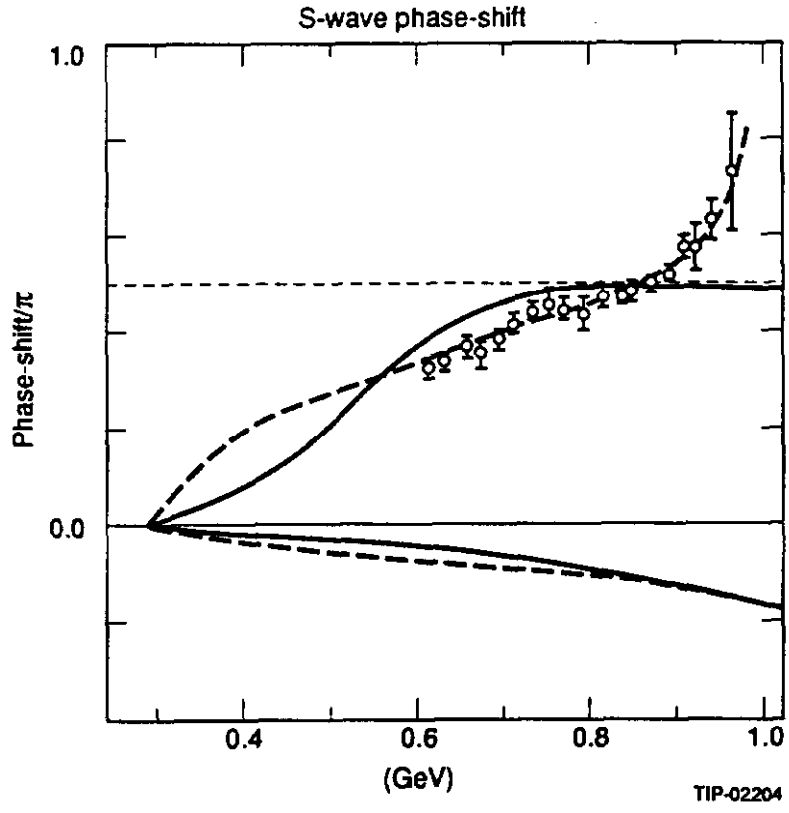

Figure 1. The σ Model Computation of I=0 and I=2 S-Wave Phase-Shifts (Solid Lines) are Compared With the Available Experimental Data.[10] The dotted line is an extrapolation of the experimental data to the threshold using the Roy equation.

3.0 RENORMALIZATION SCHEMES

First note that m_H and λ are related by

$$\lambda = \frac{m_H^2}{2v^2}. \tag{5}$$

Thus once one is renormalized, the value of the other is predicted. In the on-shell (OS) subtraction scheme, the physical Higgs mass, i.e. the position of the pole of the propagator, is an input. In the mass-independent (MI) subtraction scheme, one introduces a renormalization constant for λ, defined at some energy scale μ, such that a simple β function can be obtained.

In this section, we shall describe the Higgs propagator in two subtraction schemes corresponding to

1. Dawson-Willenbrock: On-shell subtraction scheme;

2. Basdevant and Lee: Mass-independent subtraction scheme.

Understanding the precise difference is crucial in cross-checking the results.

3.1 On-shell Subtraction Scheme

The loop contributions to the Higgs self-energy are given by

$$\lambda\Pi(s) = \frac{\lambda m_H^2}{8\pi^2} Q_2(x) \,, \tag{6}$$

where

$$x = \frac{s}{m_H^2} \,, \tag{7}$$

and

$$Q_2(x) = \tfrac{3}{2}[\log(-x) + 3I(x) + 6 - \pi\sqrt{3}] \,. \tag{8}$$

The integral $I(x)$ can be written:

$$\begin{aligned} I(x) &= \int_0^1 dt \log[1 - xt(1-t)] \\ &= \sqrt{\frac{x-4}{x}} \log \frac{\sqrt{4-x} + \sqrt{-x}}{\sqrt{4-x} - \sqrt{-x}} - 2 \,. \end{aligned} \tag{9}$$

To first order in λ, the Higgs propagator is

$$\Delta_H(s) = \frac{1}{s - m_H^2} + \frac{\lambda\Pi(s)}{(s - m_H^2)^2} \,. \tag{10}$$

This expression has a second-order pole at $s = m_H^2$, which is not correct physically. The standard way out of this difficulty is to sum an infinite number of bubbles:

$$\Delta_H(s) = \frac{1}{s - m_H^2 - \lambda\Pi(s)} \,. \tag{11}$$

This function has the expected pair of conjugate simple poles on secondary Riemann sheets. At $s = m_H^2$, the real part of this function vanishes and its imaginary part is proportional to m_H^{-4}.

Note that the mass counter-term was introduced in the lagrangian so that

$$\mathrm{Re}(\Delta_H^{-1}(m_H)) = 0. \tag{12}$$

3.2 Mass-Independent Subtraction Scheme

The σ propagator given by BL is:

$$D^{-1}(s) = s - M_s^2 - \lambda\Pi(s), \tag{13}$$

where

$$\Pi(s) = M_s^2 \left\{9\bar{B}_{\sigma\sigma}(s) + 3\bar{B}_{\pi\pi}\right\}, \tag{14}$$

with

$$\bar{B}_{xy} = B_{xy} - B_0, \tag{15}$$

$$B_{xy}(k^2) = i\int \frac{d^4p}{(2\pi)^4}\frac{1}{p^2-\mu_x^2}\frac{1}{(k-p)^2-\mu_y^2}. \tag{16}$$

B_0 arises from the counter terms in the lagrangian. If one defines a divergent integral such as Eq. (16) by dimensional regularization, one can set

$$B_0 = -\frac{1}{16\pi^2}\frac{1}{\epsilon}. \tag{17}$$

With this choice, simple mass-independent renormalization group equations can be derived.

BL in their work adopt the following definition:

$$B_0 = i\int \frac{d^4p}{(2\pi)^4}\left(\frac{1}{p^2-m_\pi^2}\right)^2. \tag{18}$$

In our work we propose a slightly different regularization prescription:

$$B_0 = i\int \frac{d^4p}{(2\pi)^4}\left(\frac{1}{p^2-\mu^2}\right)^2 \equiv -\frac{1}{16\pi^2}\left(\frac{1}{\epsilon} - \gamma + \log 4\pi\right) + \frac{1}{8\pi^2}\log\mu\,, \tag{19}$$

which reduces to Eq. (18) in the case $\mu = m_\pi$. In this way we obtain the same beta function as in the usual renormalization method (see Section 5). We thus loosely call Eq. (19) the mass-independent subtraction prescription.

3.3 The Relationship Between OS and MI

We now discuss the relationship between the OS and MI subtraction schemes. In the $m_\pi = 0$ limit, BL obtained

$$f_\pi^2 = v^2 \left(1 + \frac{\lambda_{MI}}{16\pi^2}\right). \tag{20}$$

The self-energy can then be written in terms of $M_s^2 = 2\lambda_{MI} f_\pi^2$ as

$$\Pi_{MI}(s) = \frac{1}{8\pi^2} M_s^2 \left\{ \frac{3}{2} \log\left(\frac{-s}{M_s^2}\right) + \frac{9}{2} I\left(\frac{s}{M_s^2}\right) + \left(12 \log \frac{M_s}{\mu} - 7/2\right) \right\}. \tag{21}$$

Note that if we set

$$\lambda_{MI} = \lambda \quad \text{and} \quad M_s = m_H \quad \text{at} \quad \mu = m_H \, \exp\left(\frac{\sqrt{3}}{8}\pi - \frac{25}{24}\right), \tag{22}$$

we obtain

$$\Pi_{MI}(s) = \frac{1}{8\pi^2} m_H^2 \left\{ \frac{3}{2} \log\left(\frac{-s}{m_H^2}\right) + \frac{9}{2} I\left(\frac{s}{m_H^2}\right) + \left(9 - \frac{9\pi}{2\sqrt{3}}\right) \right\}. \tag{23}$$

and then Π_{MI} coincides with Π (see Eq. (6)): thus Eq. (22) gives the OS subtraction scheme in terms of the MI subtraction scheme.

With this procedure to go from one renormalization prescription to the other, we can check for the consistency of the two computational schemes.

4.0 SECOND-ORDER RESULTS

In terms of the Mandelstam variables s, t, and u, we define the dimensionless quantities

$$x = \frac{s}{m_H^2} \qquad y = \frac{t}{m_H^2} \qquad z = \frac{u}{m_H^2} \tag{24}$$

with $x + y + z = 0$. To order λ, the $W_L^+ W_L^- \to Z_L Z_L$ amplitude is

$$M_0(\lambda, x) = \frac{2\lambda x}{1 - x}. \tag{25}$$

We write the order λ^2 contribution, in the on-shell formalism, in the form

$$M_1(\lambda, x, y) = \frac{2\lambda^2 x}{(1-x)^2} P(x, y, -x-y) \tag{26}$$

where, following the analysis of Dawson and Willenbrock,[6] we split up the function P into 6 terms:

$$P(x,y,z) = -\frac{1}{8\pi^2 x}\sum_{i=1}^{6} Q_i \,. \tag{27}$$

Notice that the x in the denominator here is cancelled by an x in the numerator in Eq. (26). It is included to emphasize the fact that $M_1(\lambda,x,y)$ tends to zero as $x \to 0$ (in fact faster than x).

The Q's come respectively from the wave-function renormalization constant, the 2-point function, the 3-point function, the bubble diagrams, the triangle diagrams and the box diagrams: they correspond precisely to the six terms in Eq. (2.31) of Ref. 6, and so we shall not reproduce them here.

4.1 Higgs Propagator and Padé Approximation

The contribution of the Higgs propagator to the $W_L^+W_L^- \to Z_LZ_L$ amplitude is

$$\overline{M} = -2\lambda m_H^2 \Delta_H(s)\,; \tag{28}$$

and with use of Eq. (10) for the propagator, $\overline{M}$ up to and including λ^2 is

$$\overline{M}_0 + \overline{M}_1 = -\frac{2\lambda m_H^2}{s-m_H^2} - \frac{2\lambda^2 m_H^2 \Pi(s)}{(s-m_H^2)^2}\,.$$

The bars indicate that these are not the full sigma-model first- and second-order terms, but only the propagator contributions. The second-order term has a double pole. However, the $[1,1]$ Padé approximant of this expression is

$$\begin{aligned}\overline{M}^{[1,1]} &= \frac{\overline{M}_0}{1-\overline{M}_1/\overline{M}_0} \\ &= \frac{-2\lambda m_H^2}{s-m_H^2-\lambda\Pi(s)}\,,\end{aligned} \tag{29}$$

which has a pair of simple poles, and is in fact exactly the same answer one would have obtained by substituting the infinite sum Eq. (11) into Eq. (28).

This is not the end of the story, since the full amplitude to order λ contains a contact term as well as the Higgs propagator, giving

$$M_0 = -2\lambda - \frac{2\lambda m_H^2}{s - m_H^2} = \frac{-2\lambda s}{s - m_H^2} \,. \tag{30}$$

The complete [1, 1] Padé approximant can be written

$$\begin{aligned} M^{[1,1]} &= \frac{M_0}{1 - M_1/M_0} \\ &= \frac{-2\lambda s}{s - m_H^2 + (s - m_H^2)^2 M_1/(2\lambda s)} \,, \end{aligned} \tag{31}$$

where M_1 is the full second-order amplitude. This contains $\overline{M}_1$, from the propagator, and so has a double pole, but it also contains many other terms. Notice that, if one were to replace M_1 here by $\overline{M}_1$, there would be problems at $s = 0$, since $\overline{M}_1$ is not zero at $s = 0$, indeed it diverges logarithmically. This would lead to an amplitude behaving like $s^2/\log s$ at threshold, which is wrong. However, the complete second-order amplitude, M_1, behaves like $s^2 \log s$ as $s \to 0$, which means that the threshold behavior of the Padé approximant Eq. (31) is the same as that of the first-order contribution, namely $2\lambda s/m_H^2$.

Dawson and Willenbrock[6] observed that M_1 has a double pole at $s = m_H^2$: they suggested the *ad hoc* replacement of the first two terms in the perturbation series—Eq. (10)—by the infinite sum of bubbles—Eq. (11)—but only when s is close to the Higgs mass. The difficulty is that use of Eq. (11) for small s values destroys the threshold behavior, $2\lambda s/m_H^2$. Thus the above authors were led a procedure of using Eq. (10) for small s—to maintain the correct threshold behavior—but Eq. (11) for larger values of s in order to remove the unwanted double pole. As we have seen, the [1, 1] Padé approximant automatically takes care of both the threshold and the pole in a unified manner.

The Spence functions that are needed for the calculation of the box and triangle diagrams were computed in a FORTRAN program using the algorithm of 't Hooft and Veltman.[7]

In the discussion of the [1,1] Padé approximant in Section 3, $M^{[1,1]}$ in Eq. (31) is a function of s and t. For technical reasons, in the calculation of phase-shifts it is more convenient first to project on to the pure isospin states ($I = 0$, 1 and 2), then to compute the first- and second-order contributions to the partial waves, and finally to make the [1,1] Padé approximation. This has two advantages:

1. The partial waves so obtained are exactly elastically unitary.

2. The occurrence of poloids is avoided (see Ref. 5 for a discussion of this point).

5.0 LANDAU GHOST AND ASYMPTOTICS

The σ model is a low energy effective theory of QCD. The phase transition from the σ model to QCD has to occur below the energy at which the model develops the Landau ghost. Thus the position of the Landau singularity gives us a rough idea of the point beyond which we can no longer trust our results.

The usual β function for L_H is

$$\beta(\lambda) \equiv \frac{\partial \log \lambda}{\partial \log \mu} = \frac{3\lambda}{2\pi^2} \tag{32}$$

to the lowest order, where μ is the renormalization point. In our mass-independent subtraction scheme,

$$\lambda_0 \equiv \lambda(1 - 12\lambda B_0) \,, \tag{33}$$

where B_0 is defined by Eq. (19). Noting that

$$\mu \frac{dB_0}{d\mu} = \frac{1}{8\pi^2} \,, \tag{34}$$

we get the same β function, Eq. (32), as in the usual momentum renormalization scheme.

The coupling runs as follows:

$$\lambda(\mu) = \frac{\lambda(\mu_0)}{1 - \frac{3}{2\pi^2}\lambda(\mu_0)\log\frac{\mu}{\mu_0}} \,. \tag{35}$$

The running coupling blows up at the Landau point, say μ_L, defined by

$$\mu_L = \mu_0 \exp\left[\frac{2\pi^2}{3\lambda(\mu_0)}\right] . \tag{36}$$

The position of the Landau ghost depends critically on the β function and thus on the details of the renormalization scheme. A somewhat more physical procedure is to look for a Landau singularity in the four-point function. Let us start with an asymptotic form of the scattering amplitude, which we can express in analytic form.

The asymptotic form of the second-order amplitude for large x and y is[8]

$$M_1(\lambda, x, y) \sim -\frac{\lambda^2}{4\pi^2}\left[4\log(-x) + \log(-y) + \log(-z) - \frac{3}{2}\pi\sqrt{3} - \frac{1}{2}\right] , \tag{37}$$

Since $t = -s(1-\cos\theta)/2$ and $u = -s(1+\cos\theta)/2$, where θ is the scattering angle, it follows from Eq. (24) and Eq. (37) that, for large $|s|$ at constant θ,

$$\mathrm{Re}M_1(\lambda) \sim -\frac{\lambda^2}{4\pi^2}\left[6\log\frac{|s|}{m_H^2} - \frac{3}{2}\pi\sqrt{3} - \frac{1}{2} + \log\frac{1-\cos^2\theta}{4}\right] . \tag{38}$$

This expression is good also for large negative values of s, where M_1 is real (the euclidean region). However, in this same limit of very large $|s|$, we see from Eq. (25) that

$$M_0(\lambda) \sim -2\lambda\,; \tag{39}$$

and so in this limit the [1,1] Padé approximant is

$$\begin{aligned} M^{[1,1]}(\lambda) &= \frac{M_0}{1 - M_1/M_0} \\ &\sim -2\lambda\left[1 - \frac{\lambda}{8\pi^2}\left(6\log\frac{|s|}{m_H^2} - \frac{3}{2}\pi\sqrt{3} - \frac{1}{2} - \log\frac{4}{1-\cos^2\theta}\right)\right]^{-1} . \end{aligned} \tag{40}$$

The asymptotic expression Eq. (37) holds in all directions in the complex s-plane, in particular for real, negative s. This means that a pole is unavoidable in this euclidean region: the redoubtable *Landau ghost*. According to the asymptotic estimate, this occurs at the point $s = -m_L^2$, where

$$m_L = m_H \exp\left[\frac{4\pi^2 v^2}{3m_H^2} + \frac{\pi}{8}\sqrt{3} + \frac{1}{24} + \frac{1}{6}\log 2\right] . \tag{41}$$

This expression is obtained from the lowest point at which the denominator in Eq. (40) is zero: this occurs at $\cos\theta = 0$. We have also used Eq. (5) to eliminate λ in favor of m_H.

Of course this estimate is approximate: it is only trustworthy for large values of m_L. To improve on it, we simply return to the Padé result itself [Eq. (31) and Eq. (26)] which gives

$$(s - m_H^2)M^{[1,1]}(\lambda) = \left[1 - \frac{\lambda}{1-x}P(x, y, -x-y)\right]^{-1} . \tag{42}$$

A pole occurs at the euclidean point, say $x = x_L < 0$, at which

$$\lambda = \frac{1 - x_L}{P(x_L, -x_L/2, -x_L/2)} . \tag{43}$$

The strategy for finding m_L is as follows:

- Choose an $x_L < 0$.
- Calculate λ from Eq. (43).
- Set $m_H = v\sqrt{2\lambda}$.
- Deduce $m_L = m_H\sqrt{-x_L}$.

In Figure 2 we show the ghost mass, m_L, plotted against the Higgs mass, m_H, according to the above calculational scheme, as well as the asymptotic curve corresponding to Eq. (41).

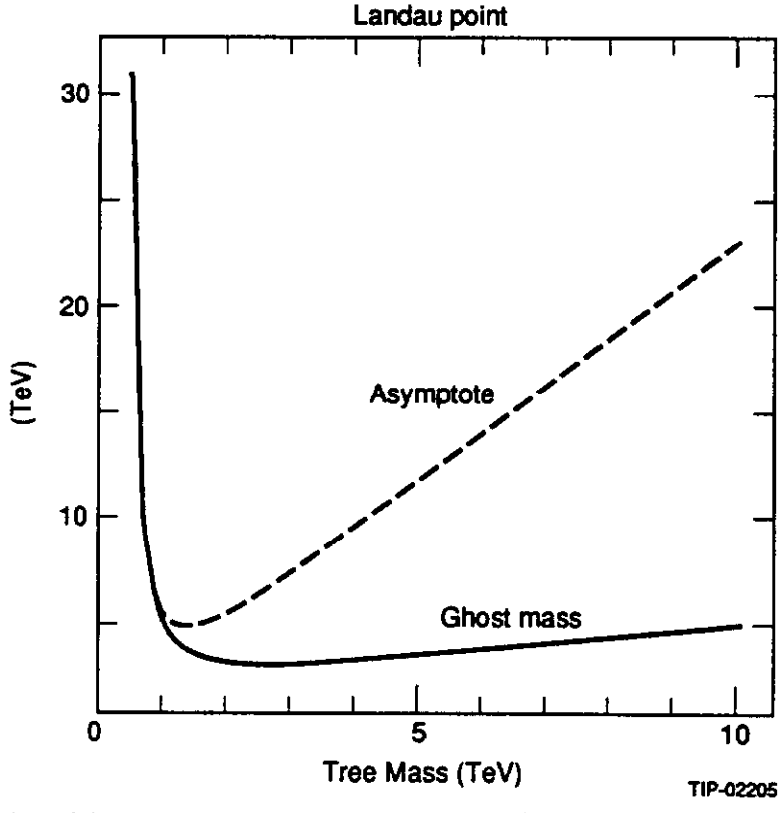

Figure 2. The Position of the Landau Ghost Obtained from Eq. (43) and That Obtained from the Asymptotic Formula (41) are Shown.

A cut-off below the Landau-ghost position could be used in order to make sense of the model. Alternatively, we can work without a cut-off, but with the proviso that only those features—like resonances—that occur well below the Landau mass m_L are to be taken seriously.

5.1 Where Can We Trust Our Results?

In our calculation, we investigated the possibility that the Higgs is heavy—or, equivalently, the coupling λ is large. It is, therefore, important to have some quantitative measure which can be used to determine the accuracy of our results. We shall show here that for the output obtained using the MI renormalization scheme, a quantitative test can be devised.

We know that physical quantities cannot depend on the renormalization point, μ. Table 1 shows the μ-dependence of $\lambda, m_H, \Gamma_H, m_\rho, \Gamma_\rho$ and the position of the Landau singularity determined from Eq. (36). For each box, λ_0 and μ_0 are given: they were determined by matching the results from the OS renormalization scheme, with use of Eq. (22). The results for two other representative values of μ are also displayed. It can be seen that results for m_H below 1 TeV are reasonably μ-independent. Around 1 TeV and above, the μ-dependence becomes severe and the trustworthiness of our results is then marginal. In Figure 3, we show the μ-dependence of the S and P wave phase-shifts for $m_H = 0.5$ and 1 TeV.

Table 1. μ-Dependence of σ Model Parameters in the Mass-Independent Subtraction Scheme. All quantities are in TeV except λ, which is dimensionless.

μ	λ	m_H	$\Gamma_H/2$	m_ρ	Γ_ρ	Landau point
.25	1.817	.50	.03	3.85	.02	
μ_0=.35	λ_0=2.0	.50	.03	4.42	.02	9.35
.45	2.169	.50	.03	4.16	.02	
.40	3.805	.73	.08	3.14	.04	
μ_0=.522	λ_0=4.5	.75	.09	3.41	.06	2.25
.60	4.970	.76	.09	3.56	.07	
.60	6.771	.96	.16	2.90	.11	
μ_0=.697	λ_0=8.0	1.00	.18	2.99	.12	1.59
.80	9.618	1.06	.21	3.05	.14	

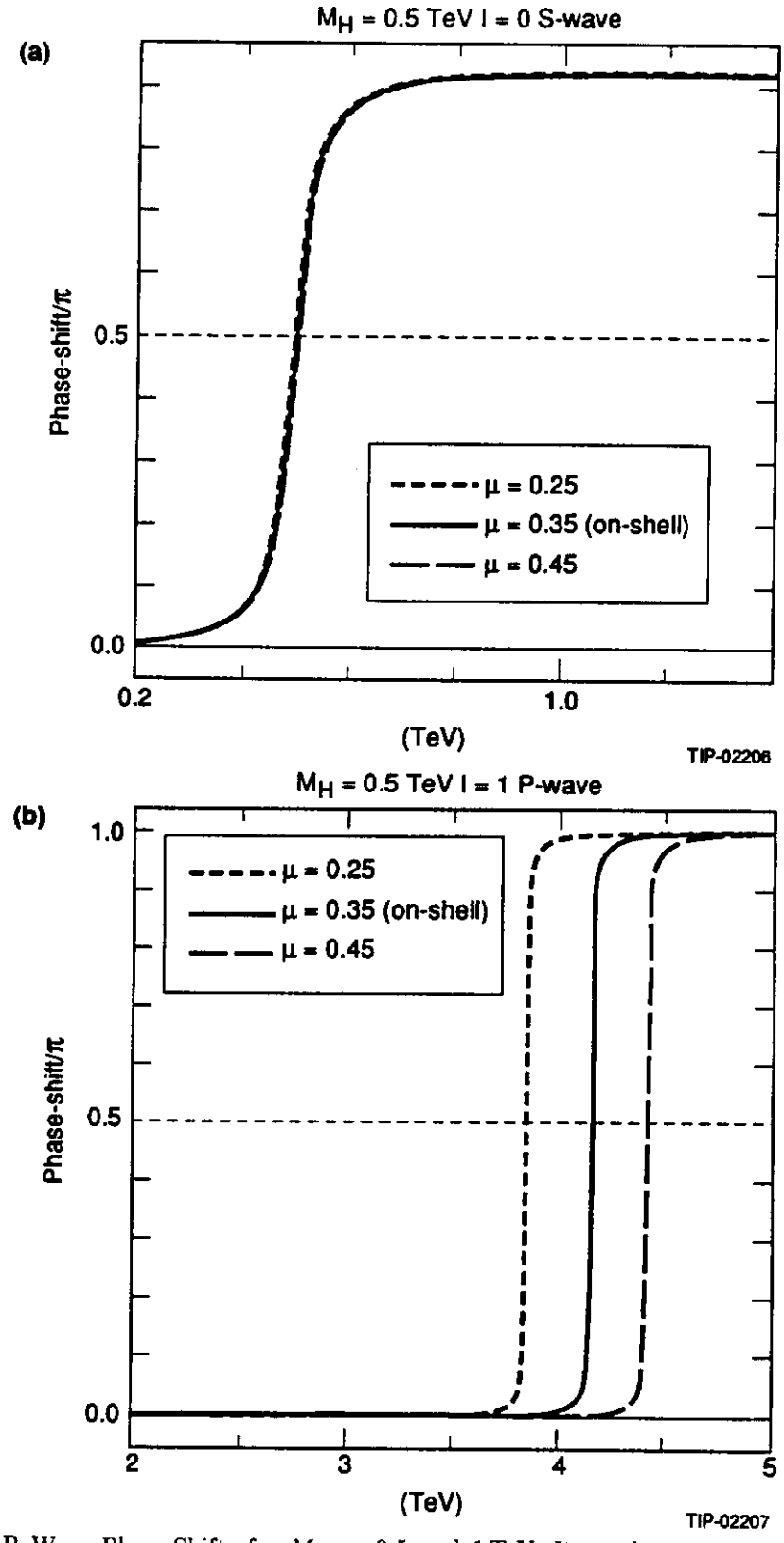

Figure 3. S and P Wave Phase-Shifts for $M_H = 0.5$ and 1 TeV. It can be seen that there is very little μ-dependence for $M_H = 0.5$ TeV. For $M_H = 1$ TeV, a considerable μ-dependence begins to appear.

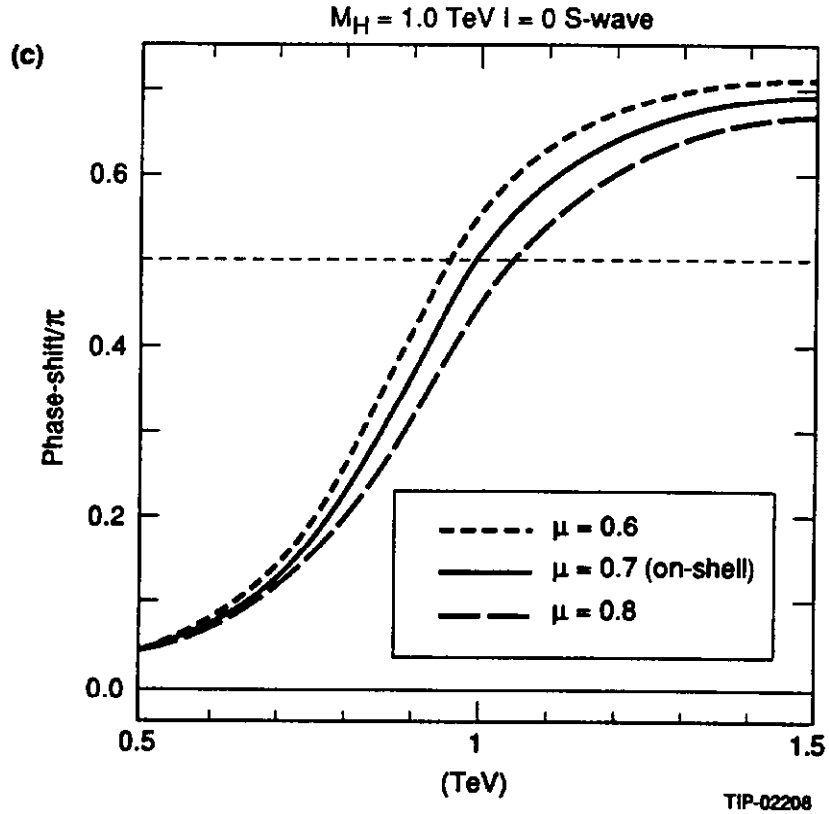

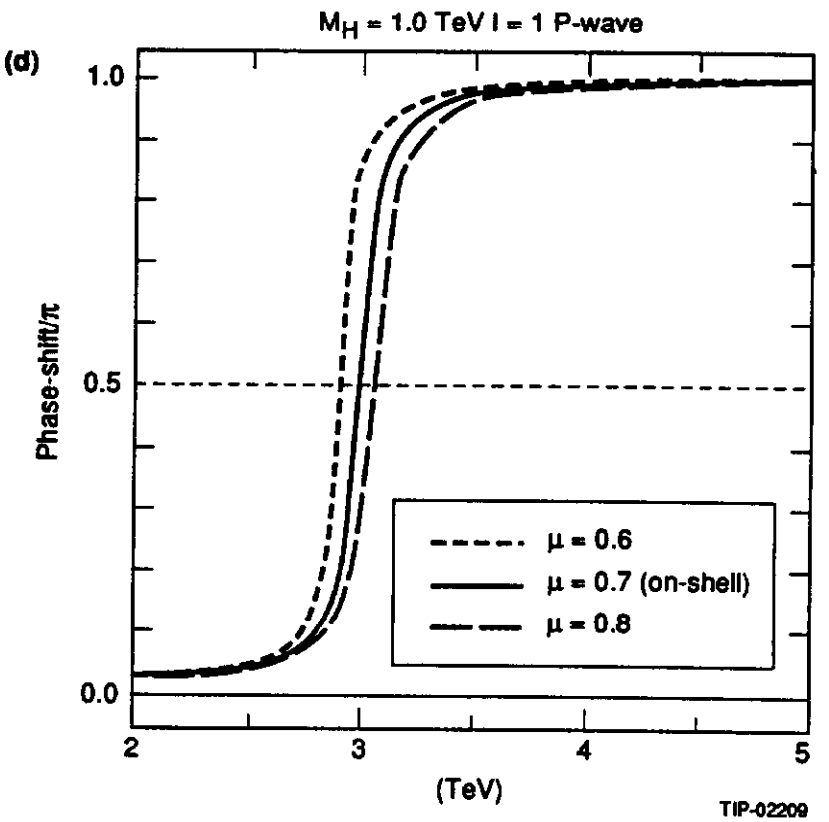

Figure 3 (Cont.)

In Figure 4, we show the μ-dependence of the S and P wave phase-shifts from which BL have computed the mass of the ρ meson.[5] There is considerable μ-dependence in the results. This finding, together with the fact that we can never obtain such a light ρ using the OS renormalization scheme, validates our conclusion that the BL result is an artifact of the Padé approximation.

Let us examine the origin of the μ-dependence shown in Table 1. The main source of the variation is the sharp variation of $\lambda(\mu)$, when μ_0 is close to the position of the Landau ghost, μ_L. The position of the Landau ghost is controlled by the β-function, and is highly dependent on the renormalization scheme. The μ-dependence shown in Table 1 applies only for the MI subtraction scheme. In particular, the results shown in Table 1 do not invalidate the results obtained by the OS renormalization scheme.

To what extent can we trust the results obtained by the OS renormalization scheme? At any rate, when the results obtained from OS and MI schemes agree, they are trustworthy (i.e. results below 1 TeV). Also, as seen in Figure 2, the Landau singularity obtained in the previous section never dips below 3 TeV. Hence we can be reasonably sure that when the energy is sufficiently smaller than 3 TeV, the OS results can be trusted.

5.2 Results

With the provisos mentioned in the previous section, we present the results of the OS renormalization scheme. In Figure 5 we show typical results for the $I = 0$ and $I = 2$ S-wave, and the $I = 1$ P-wave phase-shifts, corresponding to a Higgs mass of 1 TeV. The $I = 0$ S-wave carries the Higgs resonance as a broad, asymmetrical peak. The phase-shift goes through $\frac{\pi}{2}$ at $\sqrt{s} = m_H$, and it is convenient to define the lower half-width to be the energy difference between the $\frac{\pi}{4}$ and the $\frac{\pi}{2}$ points. For example with $m_H = 1$ TeV this half-width is 0.18 TeV. The $I = 2$ S-wave is small and repulsive, as expected. The $I = 1$ P-wave has a sharp, symmetrical resonance, and we define its mass by the $\frac{\pi}{2}$ point, the full width by the energy-difference between the $\frac{\pi}{4}$ and the $\frac{3\pi}{4}$ points. The 'rho' mass and full width are in this case 2.99 TeV and 0.12 TeV respectively.

These masses and widths have been calculated for a number of input tree masses; in Figure 6 we display these parameters up to 5 TeV tree mass. Note that, in the on-shell formalism, the output Higgs mass is equal to the tree mass below about 2.6 TeV: above that point it is smaller. The reason is that, although the subtraction scheme guarantees that the real part of the $I = 0$ S-wave amplitude vanishes at $s = m_H^2$, there is a second point at which this happens, and when $m_H > 2.6$ TeV, this point is actually lower than m_H.

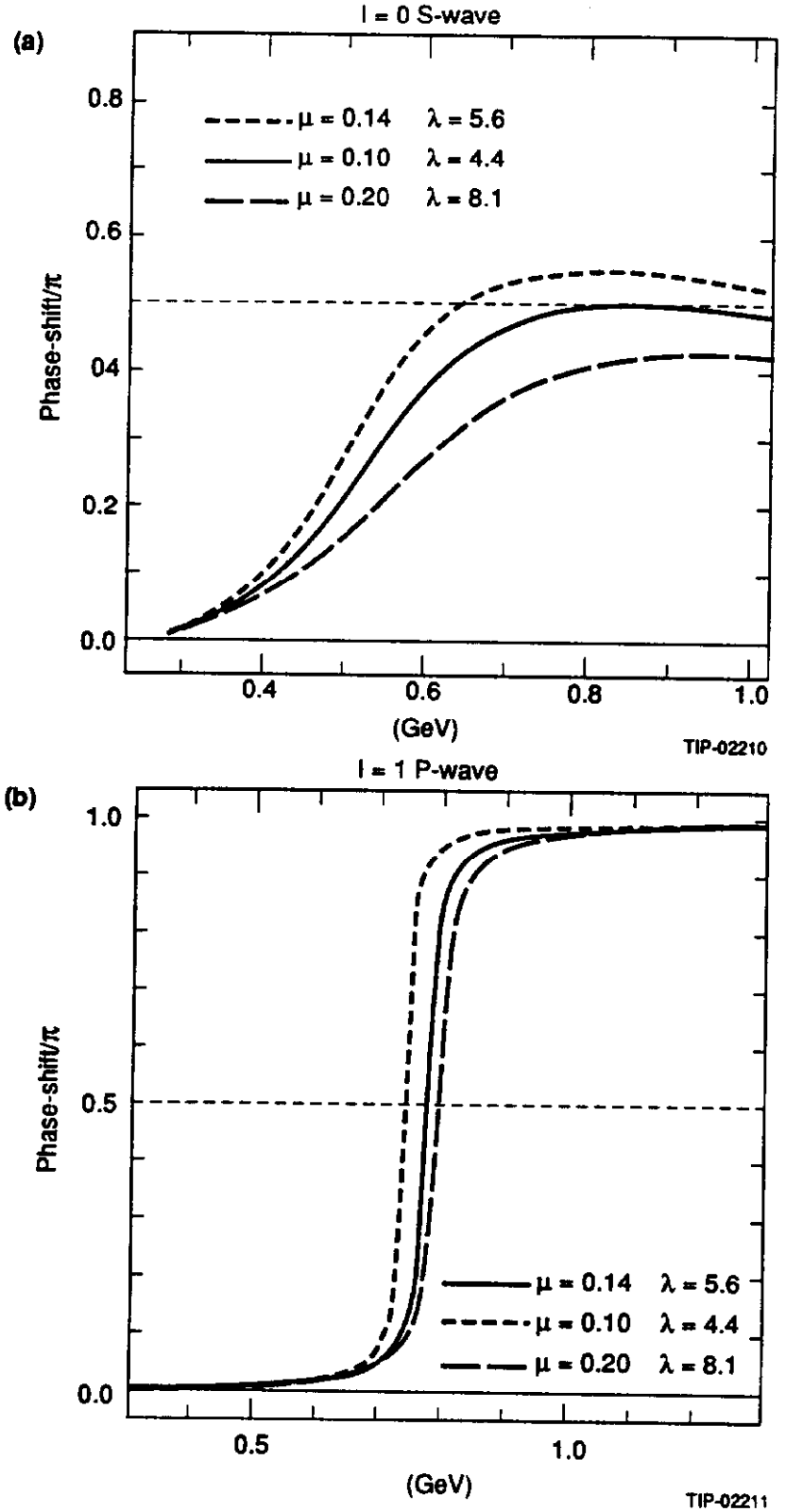

Figure 4. The μ-Dependence of the I=0 S Wave and I=1 P Wave Phase-Shifts for the Set of Parameters Which Yields the Result of Basdevant and Lee Shown in Eq. (1). There is a considerable dependence on the renormalization point. We also emphasize that this result cannot be reproduced if the on-shell renormalization scheme is used.

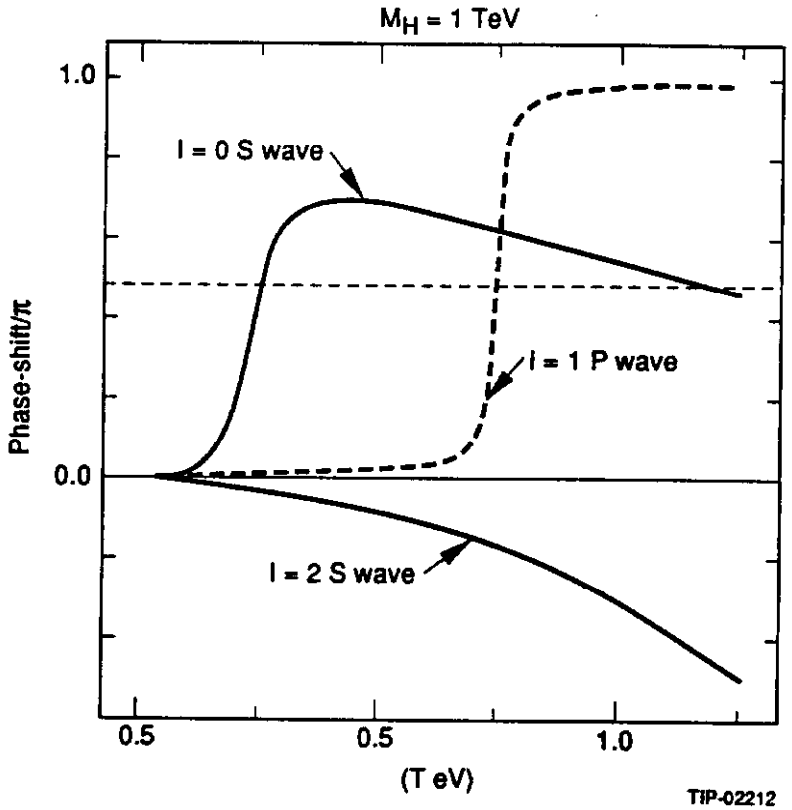

Figure 5. A Typical Phase-Shift Obtained for $M_H = 1\,\text{TeV}$, Using the On-Shell Renormalization Scheme.

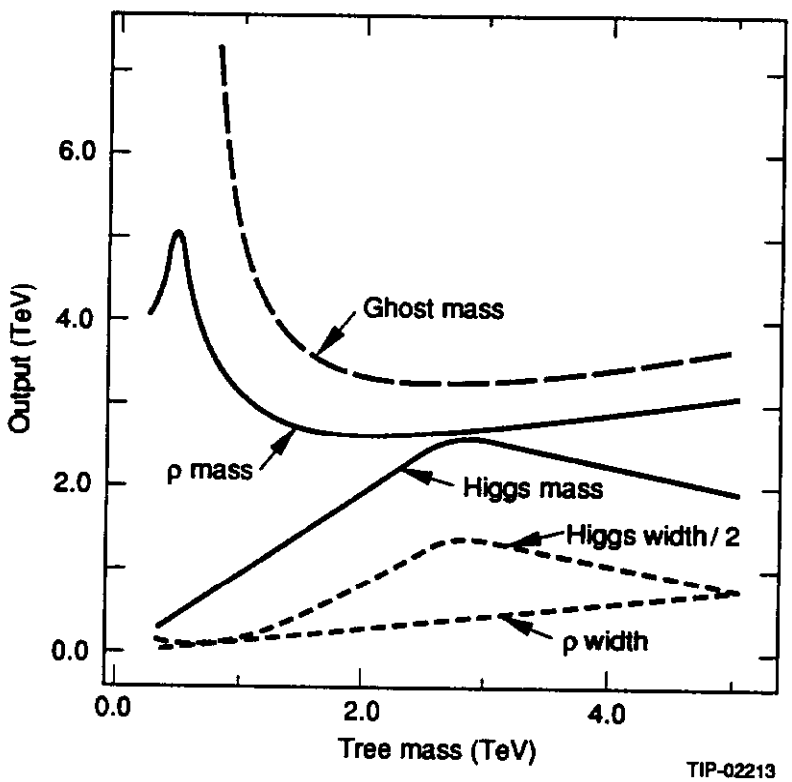

Figure 6. The Mass and the Width are Shown as Functions of the Input Tree Mass, Using the On-Shell Renormalization Scheme. The position of the Landau singularity is also shown.

The 'rho' mass is never less than 2.6 TeV, this minimum being reached when the Higgs mass is 2 TeV. In the following section we will discuss what significance such a high mass can have, since an effective theory must essentially be cut off, in view of the occurrence of a Landau ghost.

6.0 CONCLUSIONS

In this paper, we have studied the simplest Higgs lagrangian in order to search for effects which can be detected at SSC. In particular, we are interested in an alternative to a Higgs search, should the Higgs be too heavy to be detected.

We have used the well-known isomorphism between the Higgs lagrangian and the O(4) σ model. The latter has been studied quite extensively in the literature. In particular, Basdevant and Lee have claimed that $\pi\pi$ resonances are generated dynamically. If substantiated, this claim would, after scaling to the TeV domain, have interesting consequences for SSC. In view of the fact that it is much easier to detect the ρ meson than the σ resonance in $\pi\pi$ scattering, we pointed out that a P-wave WW resonance is likely to be seen before a Higgs with mass above 800 GeV is detected.

Our first step was to check the result of Basdevant and Lee. We could indeed reproduce their results; but the value of the coupling constant (defined at m_π) needed to produce their effect is unacceptable. In fact for their value of coupling constant, the Landau ghost sits between m_π and m_ρ! For this reason, a slight change in the renormalization point changes the coupling constant considerably; and it also changes the mass of the ρ. We have shown that m_ρ can never be below 1 GeV.

We have computed the $\pi\pi$ phase-shifts and compared them with experiment. The agreement between theory and experiment is reasonable for the S waves, considering the fact that we have confined ourselves only to the [1,1] Padé approximation. The P wave phase-shift agrees qualitatively with experiment: quantitatively it is however unsatisfactory, since it is resonant only at 1 GeV.

The agreement between theory and experiment for the S-wave phase-shift up to 1 GeV gives us the courage to trust the σ model predictions up to about that energy. Thus we can be confident that the *absence* of a resonance at $\sim m_\rho = 760$ MeV is a reliable result. This implies that other particles must be added in order to construct an accurate low-energy effective theory of QCD. The fate of our P-wave resonance around 1 GeV is not clear: perhaps kaon or nucleon loops will pull its mass down to m_ρ; but it may be that the resonance is largely created by exchange of the other particles, and that our 1 GeV effect

is a Padé artifact. We expect that the introduction of more massive states will not change the prediction for the S-wave phase-shift by more than 10%.

Turning to our predictions for the Higgs model: from Figure 6 one can read off the mass of the P-wave WW resonance ρ_W as a function of m_H. Our picture becomes suspect around $m_H \sim 2.5\,\mathrm{TeV}$. In the same figure, we also show the width of the ρ_W. Note that

$$\Gamma_{\rho W} \;<\; \frac{\Gamma_H}{2}. \tag{44}$$

While the vector state is considerably heavier (1.5~4 times) than is the scalar one, its narrowness may make it detectable. We can be confident that the σ model *predicts the absence of a P-wave resonance below 2 TeV;* conversely, the experimental discovery of such a state would definitely imply violation of the standard model and would consequently herald new physics.

ACKNOWLEDGEMENTS

We would like to thank M. Tanabashi, T. Truong and K. Yamawaki for discussions. M. Tanabashi was involved in the early stage of this collaboration. This work is supported in part by U.S. Department of Energy, Grant Number DOE-AC02-87ER-40325.TASKB.

REFERENCES

1. J. Shigemitsu Nucl. Phys. (*Proc. Suppl.*) **20**, 515 (1991), and references therein.
2. R. Dashen and H. Neuberger, Phys. Rev. Lett. **50**, 1897 (1983).
3. This has in fact been attempted in an extended electroweak theory, see R. Casalbuoni, P. Chiappetta, S. De Curtis, F. Feruglio, R. Gatto, B. Mele and J. Terron, Phys. Lett. **B249**, 130 (1990). See also M. Bando, T. Kugo, S. Uehara, K. Yamawaki, and T. Yanagida, Phys. Rev. Lett. **54**, 1215 (1985).
4. Kobayashi and Matsuki commented briefly on a similar possibility, see M. Kobayashi and M. Matsuki, High-energy Physics-1980 (20th International Conference. Madison. Wisconsin) Part 1. p. 440, while Rosenfeld investigated the scenario by means of a unitarization of the tree amplitude: R. Rosenfeld, Phys. Rev. **D42**, 126 (1990).
5. J.L. Basdevant and B.W. Lee, Phys. Rev. **D2**, 1680 (1970).
6. S. Dawson and S. Willenbrock, Phys. Rev. **D40**, 2880 (1989). See also W. Marciano and S. Willenbrock, Phys. Rev. **D37**, 2509 (1988), and D.A. Dicus and W.W. Repko, Phys. Rev. **D42**, 3660 (1990).
7. G. 't Hooft and M. Veltman, Nucl. Phys. **B272**, 1232 (1986).
8. For example at $x = 50000$ and $y = -20000$, this formula gives

$$M_1(\lambda, x, y) \approx (-0.34721, 0.079577) ,$$

whereas the FORTRAN program produces, for the full calculation,

$$M_1(\lambda, x, y) \approx (-0.34723, 0.079554) .$$

9. M. Chanowitz and M.K. Gaillard, Nucl. Phys. **B261**, 379 (1985).
10. "Review of Particle Properties", Phys. Lett. **B239** (1990); see also B.R. Martin, D. Morgan and G. Shaw, "Pion-Pion Interactions in Particle Physics", Academic Press (1976).

APPENDIX A

In this appendix, we shall describe the essential point of the equivalence theorem without going into the details (see Ref. 9 for a proof). Consider a gauge boson propagator in the unitary gauge:

$$\Delta_{\mu\nu}(q) = \frac{g_{\mu\nu} - \frac{q_\mu q_\nu}{M_W^2}}{q^2 - M_W^2} \,. \tag{45}$$

We can split up this propagator into the longitudinal and transverse pieces:

$$\Delta_{\mu\nu}(q) = \frac{g_{\mu\nu} - \frac{q_\mu q_\nu}{q^2}}{q^2 - M_W^2} - \frac{1}{M_W^2}\frac{q_\mu q_\nu}{q^2} \tag{46}$$

The second term can be interpreted as an exchange of a massless scalar boson with wrong statistics ($-$ sign). It is accompanied by two kinematical factors $\frac{q_\mu}{M_W}$ which change the spin-one coupling of a vector boson to a spin-0 coupling of a Nambu-Goldstone boson at both ends of the propagator. Now the W boson fusion process shown in Figure 7 can be split into four pieces. Figure 8 represents a fusion of two massless Nambu-Goldstone bosons. This fusion process is given by:

$$\frac{q_{1\alpha}}{M_W}\frac{q_{2\beta}}{M_W}T^{\alpha\beta} \approx \epsilon_{1\alpha}^L \epsilon_{2\beta}^L T^{\alpha\beta} \,. \tag{47}$$

At high energies the longitudinal polarization of a spin-one particle is $\frac{q^\mu}{M}$, so the above represents the scattering amplitude for on-shell longitudinally polarized gauge bosons. Thus if Figure 8 dominates over the other three graphs, the amplitude for WW scattering is dominated by that of $W^L W^L$ scattering, which in turn is equal to the Nambu-Goldstone boson scattering amplitude. Now, if the self-coupling of Nambu-Goldstone boson is strong, Figure 8 will indeed dominate over the other diagrams, since they are suppressed by the gauge coupling constants. Note that the above argument applies only when the gauge boson masses can be neglected compared to their energies.

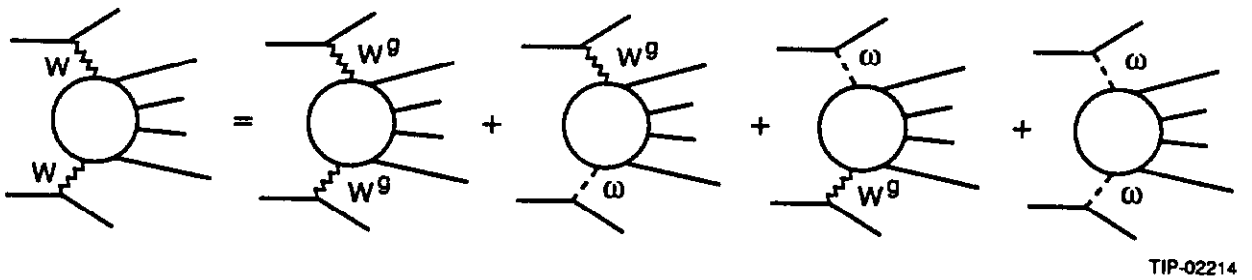

Figure 7. Diagrams that Contribute to WW Scattering.

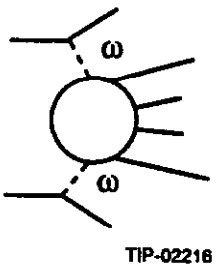

Figure 8. If the Coupling in the Higgs Sector is Large, the Nambu-Goldstone Boson Scattering Dominates Over the Four Diagrams Shown in Figure 7.